Spin Accumulation in Forward-Biased MnAs/GaAs Schottky Diodes

J. Stephens,[1] J. Berezovsky,[1] J. P. McGuire,[2] L. J. Sham,[2] A. C. Gossard,[1] and D. D. Awschalom[1]
[1]*Center for Spintronics and Quantum Computation, University of California, Santa Barbara, California 93106, USA*
[2]*Department of Physics, University of California San Diego, La Jolla, California 92093-0319, USA*
(Received 10 January 2004; published 27 August 2004)

We describe a new means for all-electrical generation of spin polarization in semiconductors. In contrast with spin injection of electrons by tunneling through a reverse-biased Schottky barrier, we observe accumulation at the metal-semiconductor interface of forward-biased ferromagnetic Schottky diodes, which is consistent with a theory of spin-dependent reflection off the interface. Spatiotemporal Kerr microscopy is used to image the electron spin and the resulting dynamic nuclear polarization that arises from the nonequilibrium carrier polarization.

DOI: 10.1103/PhysRevLett.93.097602 PACS numbers: 76.70.Fz, 72.25.Dc, 75.70.–i, 78.47.+p

The injection of electrons from ferromagnetic metals into semiconductors has recently received much attention in the field of spintronics since these systems have the potential to serve as room-temperature sources of spin polarization [1]. To date, most research in this vein has focused on electron currents flowing through a tunnel barrier from the ferromagnet (FM) to the semiconductor (SC). For example, spin injection has been observed for tunneling through Schottky [2,3] and aluminum oxide [4] tunneling barriers, as well as in more complicated structures such as magnetic tunnel transistors [5]. All of these schemes share the common feature that spin-polarized electrons are injected from the FM into the SC. In addition, the discovery of the ferromagnetic proximity polarization (FPP) effect [6,7] demonstrated a different route toward creating spin polarizations in semiconductors, but required the optical excitation of photocarriers. Here we describe a new means of electrically generating such spin polarizations in a lateral device that requires neither optical excitation nor that the sample be reverse biased.

In this Letter we report evidence of spin accumulation in ferromagnetic MnAs/GaAs Schottky diode structures biased in the forward direction [8]. In contrast with the FPP effect where no charge transport occurred, an electron current flows from the GaAs into the MnAs, and a net electron spin polarization arises in the GaAs. We use two spatially resolved techniques to map the lateral dependence of the electron spin polarization and the subsequent dynamically polarized nuclear spins. Both the electron and nuclear spin polarization profiles track the expected current density through the Schottky diode. A theory in which the spin polarization arises due to spin-dependent electron transmission and reflection at the FM-SC interface is used to estimate that the steady state spin polarization at modest forward bias in our device is a few percent [9,10].

Samples are grown by molecular beam epitaxy and consist of 25 nm type-A MnAs, 500 nm n-GaAs, and 400 nm $Al_{0.75}Ga_{0.25}As$, grown on a semi-insulating GaAs(100) substrate [11]. Using photolithography and wet etching, a $50 \times 100\ \mu m^2$ MnAs mesa is defined at the center of a channel etched into the n-GaAs layer, as shown in Fig. 1(a). A metal contact is deposited on the n-GaAs across the channel from the MnAs mesa, and annealed to form an Ohmic contact. A second contact is then deposited on the MnAs mesa, thus forming a Schottky diode in series with a resistor, which shows typical rectifying I-V characteristics. Hysteresis loops measured in a superconducting quantum interference device magnetometer demonstrate that the MnAs is ferromagnetic with a Curie temperature of ~320 K. While the data presented in this Letter are from a single sample with the n-GaAs layer Si doped at $8 \times 10^{16}\ cm^{-3}$, we have measured a number of samples with doping ranging

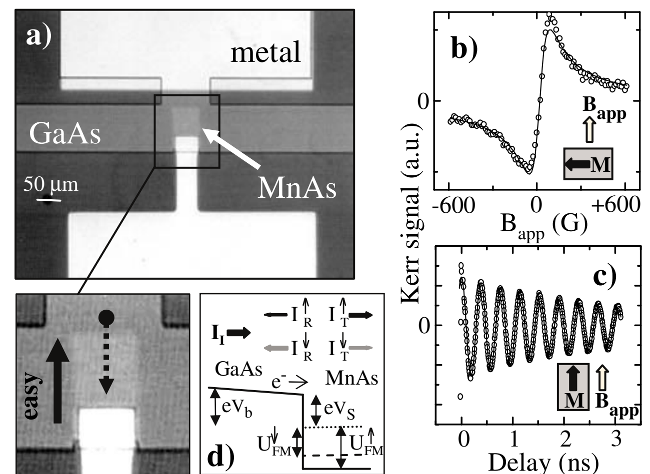

FIG. 1 (color online). (a) Charge-coupled device micrographs of spin accumulation device. Closeup depicts the MnAs magnetic easy axis direction as well as the line cut measurement path (see text). (b) Hanle-MOKE data (symbols) and fits (lines) and (c) TRKR at $T = 7.5$ K. Insets show the two measurement geometries. (d) Schematic conduction band diagram of Schottky interface for magnetization parallel to spin-up electrons. Also depicted is a cartoon of the spin-dependent incident (I_I), reflected (I_R), and transmitted (I_T) electron currents.

 © 2004 The American Physical Society

from 6×10^{16} to 1×10^{18} cm^{-3} [12]. We have also fabricated a control sample with a nonmagnetic Schottky diode in which none of the spin effects discussed here were present.

In order to probe electron and nuclear spin polarization in the GaAs epilayer, we use two different optical techniques. In each case the sample is mounted in a He flow cryostat, and laser pulses that are used to probe the spin polarization (see below) are focused on the sample through a scanning microscope objective, providing $\sim$2 μm lateral resolution [13].

To measure the electron spin, we use a hybrid of the Hanle and magneto-optic Kerr effect (MOKE) measurements, which we refer to as Hanle-MOKE. In this technique, the polarization of a linearly polarized probe beam ($\lambda \sim 812$ nm, 550 μW) is rotated upon reflection off the sample through an angle proportional to the projection along the growth direction of the time-averaged electron spin polarization. This angle is measured as an applied transverse magnetic field is swept in a small range about $B_{\rm app} = 0$. This contrasts with traditional Hanle experiments, in which the spin is detected by photoluminescence polarization. For electron spin initially polarized at $t = 0$ perpendicular to the applied field and in the plane of the sample, the MOKE signal may be written as $S(t) = A\exp(-t/\tau)\sin(\omega_L t)$, where τ is the transverse spin lifetime, $\omega_L = 2\pi\nu_L$ where ν_L is the Larmor precession frequency, and A is a scale factor. Integrating S with respect to t, one finds the time-averaged signal to be $\langle S\rangle = A\omega_L/(1/\tau^2 + \omega_L^2)$ [Eq. (1)]. Fitting the data obtained by this technique yields the spin lifetime and the parameter A, which is proportional to the spin polarization rate. The quantity $A\tau$ is then proportional to the time-averaged spin polarization in zero applied field, assuming the spin lifetime is independent of field (a good assumption for the modest fields used here).

Nonequilibrium electron spin polarization should result in the well-known phenomenon of dynamic nuclear polarization (DNP), which is due to electron and nuclear spin-flip interactions [14]. Moreover, DNP was previously observed to arise from spin injection in reverse-biased Schottky diodes [15]. To measure the nuclear polarization we use the time-resolved Kerr rotation (TRKR) technique [16]. Here, a $\sim$150 fs duration circularly polarized pump pulse ($\lambda \sim 812$ nm, 450 μW) from a mode-locked Ti:sapphire laser excites spin-polarized electrons into the conduction band of the n-GaAs. These optically injected spins then precess around a transverse magnetic field at the Larmor frequency and decay exponentially with transverse lifetime τ. A time Δt later, a linearly polarized probe pulse ($\lambda \sim 812$ nm, 350 μW) measures the instantaneous projection of the spin onto the growth direction through the Kerr effect. Scanning Δt yields an oscillatory Kerr rotation signal $\theta_K(\Delta t) \sim e^{-(\Delta t/\tau)}\cos(2\pi\nu_L\Delta t)$ from which one obtains ν_L. Through the hyperfine interaction, a net nuclear polarization acts like an effective magnetic field B_N on the electron spins; therefore, the Larmor frequency of the optically injected electrons is proportional to the sum of the applied field $B_{\rm app}$ and B_N [17]. By measuring ν_L, we obtain the effective nuclear field, which is proportional to the nuclear polarization [18].

Characteristic Hanle-MOKE and TRKR curves, along with schematics of each measurement geometry, are shown in Figs. 1(b) and 1(c) [19]. For the Hanle-MOKE measurement, the sample is mounted with the magnetocrystalline easy axis of the MnAs perpendicular to the applied field. Because of the strong uniaxial anisotropy present in MnAs, the magnetization deviates only slightly from the easy axis in the magnetic fields used in these experiments. We apply a 6 kHz square wave to the Schottky diode, oscillating between $V_b = 0$ and $+1.5$ V ($I_b = 0$ to 1.65 mA), which allows us to use lock-in detection of the electrically induced MOKE signal. Fitting the curves obtained through the Hanle-MOKE technique yields the spatial map of the time-averaged spin polarization ($A\tau$) shown in Fig. 2(a). As expected, we find that switching the magnetization of the FM yields a sign change in the Hanle-MOKE signal (not shown).

For the nuclear polarization measurements, the sample was mounted with the MnAs easy axis parallel to $B_{\rm app}$. With $B_{\rm app} = 2$ kG and a forward bias of $V_b = 1.5$ V ($I_b =$ 1.65 mA), we observe nuclear polarization under the MnAs mesa building up over the course of approximately 20 min, with a maximum effective nuclear field $B_N =$ 0.45 T and a maximum effective field gradient of 8×10^4 T/m. The sign of the effective nuclear field indicates that the electron spin is polarized antiparallel to the MnAs magnetization, in agreement with previous measurements [7]. Figure 2(b) shows an image of the resulting nuclear polarization which is in qualitative agreement with the electron polarization. Discrepancies between the images of electron and nuclear polarization may be due in part to the fact that electron spins decay with the transverse lifetime in the case of the Hanle-MOKE measurement, but the longitudinal lifetime is the relevant time scale in the DNP measurement. Sweeping the field and measuring the nuclear polarization yields a hysteresis loop similar to those previously measured [6], with a switching event occurring at the MnAs coercive field, thus confirming the role of the FM in this phenomenon.

We have used both the TRKR and Hanle-MOKE measurements to investigate the dependence of nuclear and electron spin polarizations on the forward-bias current. Figure 2(c) shows line cuts of the electron spin polarization taken along the path indicated by the dashed line in the inset of Fig. 1(a). We find no measurable electron polarization for $V_b < 0.8$ V, which corresponds to the turn-on of the Schottky diode. At higher voltages, current begins flowing and the electron polarization increases. The maxima of these curves as a function of applied bias are shown in the inset of Fig. 2(c).

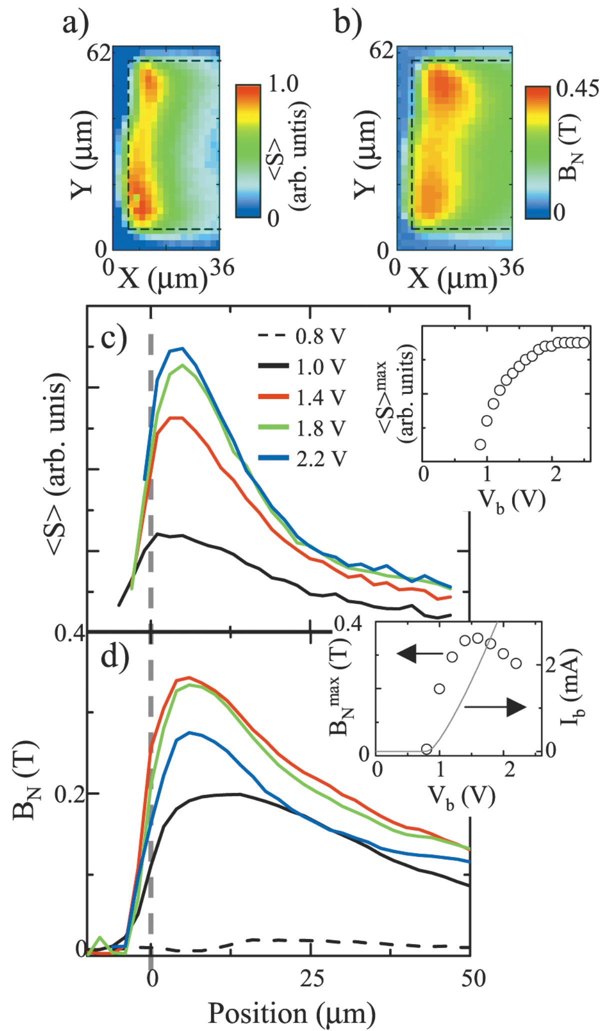

FIG. 2 (color). (a) A 2D image of time-averaged electron spin ($A\tau$) taken at $T = 7.5$ K with a square wave between 0 and 1.5 V applied at 6 kHz. (b) A 2D image of effective nuclear field B_N taken at $T = 7.5$ K with forward bias of 1.5 V and applied field of 2 kG. Dotted lines show the outline of the MnAs mesa. Line cuts of (c) ($A\tau$) for various forward biases between 0.8 and 2.2 V, and (d) B_N along the path indicated in Fig. 1(a). Insets show the peak value of each as a function of bias.

The same line cuts were measured using the TRKR technique, and the extracted nuclear spin polarization is shown in Fig. 2(d). The results closely match the electron polarization profiles. Again, the maxima of these curves are shown in the inset. One difference between the two measured spin profiles is that the nuclear polarization reaches a maximum at about $V_b = 1.6$ V and subsequently decreases at higher bias, possibly due to resistive heating.

We also performed temperature dependence measurements of both the nuclear and electron spin, the results of which are shown in Fig. 3. A TRKR measurement with optically injected spins at zero applied field was used to normalize the Hanle-MOKE results as a function of temperature since the magnitude of the Kerr effect was

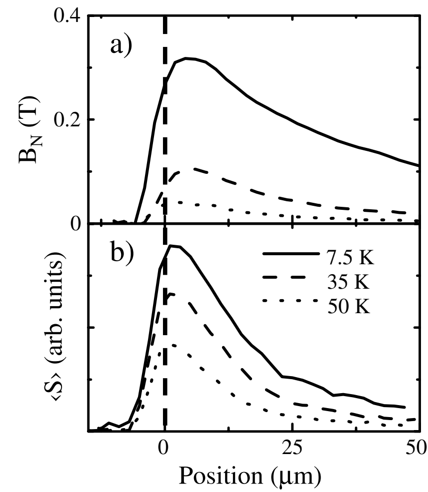

FIG. 3. Line cuts at various temperatures taken along the path shown in Fig. 1(a) of (a) effective nuclear field and (b) time-averaged electron spin from $T = 7.5$ to 50 K. Dashed vertical line indicates the position of the front edge of the MnAs mesa. For the nuclear field measurement the forward bias was 1.5 V, while for the electron spin measurement a 6 kHz square wave between 0 and 1.5 V was applied.

observed to decrease by ~30% from $T = 7.5$ to 50 K. We find that the magnitude of the nuclear polarization and the time-average electron spin polarization both decrease monotonically with increasing temperature, but that the nuclear polarization decreases more quickly. This is expected since the nuclear polarization depends not only on the average electron spin polarization but also on the nuclear relaxation time, which decreases with increasing temperature [20].

Figures 4(a) and 4(b) show the same current dependence measurements as Fig. 2(d), but with the spin accumulation rate A and spin depolarization rate $1/\tau$ plotted separately. We see that the spin accumulation rate is sharply peaked near the leading edge of the MnAs, and is quite small elsewhere under the mesa. Similarly, the spin depolarization rate is peaked at the leading edge, but then decreases to a constant value farther away. The shape of A as a function of position is similar to what one would expect for the lateral current density across the SC-FM interface, since the conductivity of the GaAs is much lower than that of the metallic MnAs. The strongly enhanced spin depolarization rate in the vicinity of the MnAs leading edge is likely due to transport of spin into the FM or away from the probe spot within the SC, an effect that will be greatest near the front of the magnetic mesa where the current density is largest. The temperature dependences of A and $1/\tau$ are shown in Figs. 4(c) and 4(d) (from the measurements of Fig. 3(b)]. Here, the spin lifetime appears to be dominated by a temperature independent contribution near the edge of the MnAs mesa, which is again consistent with the picture of spin being transported away from the probe spot in the area of high current density.

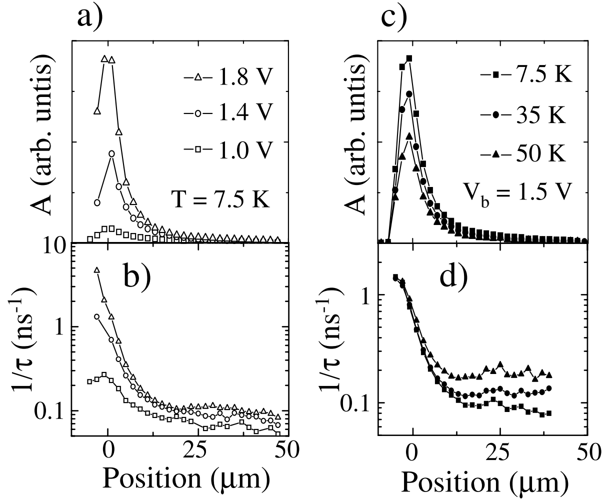

FIG. 4. Line cuts showing the bias dependence of (a) the electron spin accumulation rate A and (b) the electron spin depolarization rate $1/\tau$ taken at $T = 7.5$ K. Line cuts of A and $1/\tau$ for $T = 7.5$ to 50 K are shown in (c) and (d), respectively. The bias conditions are the same as in Fig. 3.

The observed effect may be qualitatively described by a simple model of spin-dependent reflection off the FM/SC interface [9,10]. The ferromagnet is modeled as exchange-split parabolic bands, resulting in different wave vectors in the ferromagnet for the two spin channels at a given energy [21]. The wave function matching conditions at the interface result in spin-dependent reflection and transmission coefficients for electrons incident at the interface. We consider transport across the interface under forward bias (see schematic shown in Fig. 1(d)], ignoring the spatial dependence of the current density and assuming the spin-flip time is sufficiently long such that the two spin channels are independent. Using the Drude relation, the spin polarization due to reflection can be calculated from the spin-dependent currents flowing through the interface,

$$\frac{n_\uparrow - n_\downarrow}{n_\uparrow + n_\downarrow} = \frac{\int_0^{k_f} dk_z k_z \int_0^{\sqrt{k_f^2 - k_z^2}} dk_\parallel k_\parallel (T_\uparrow - T_\downarrow)}{\int_0^{k_f} dk_z k_z \int_0^{\sqrt{k_f^2 - k_z^2}} dk_\parallel k_\parallel (T_\uparrow + T_\downarrow)}, \quad (1)$$

where k_f is the Fermi wave vector in the semiconductor, k_z is its component in the growth direction, $k_\parallel$ is the component parallel to the interface, n is the doping density, and $T_\uparrow$ and $T_\downarrow$ are the transmission coefficients for the two spin channels. Using reasonable material parameters [22] and assuming the SC spin lifetime is dominated by current flow into the FM, the theory estimates the spin polarization to be a few percent and is consistent with the observed nuclear polarization [15].

The spin accumulation effect represents a new method for electrically generating spin polarizations in semiconductors. This phenomenon may find application in future spin-based devices; in addition, the spatially resolved measurement techniques used here should prove useful in the characterization of such structures.

This work was supported by the ARO and DARPA/ONR.

[1] S. A. Wolf *et al.*, Science **294**, 1488 (2001).
[2] H. J. Zhu *et al.*, Phys. Rev. Lett. **87**, 016601 (2001).
[3] M. Ramsteiner *et al.*, Phys. Rev. B **66**, 081304(R) (2002).
[4] V. F. Motsnyi *et al.*, Appl. Phys. Lett. **81**, 265 (2002).
[5] X. Jiang *et al.*, Phys. Rev. Lett. **90**, 256603 (2003).
[6] R. K. Kawakami *et al.*, Science **294**, 131 (2001).
[7] R. J. Epstein *et al.*, Phys. Rev. B **65**, 121202(R) (2002); **68**, 041305(R) (2003).
[8] We did not observe reverse bias spin injection, probably due to the small tunneling current through the wide Schottky barrier present in the lightly doped GaAs.
[9] C. Ciuti, J. P. McGuire, and L. J. Sham, Phys. Rev. Lett. **89**, 156601 (2002).
[10] J. P. McGuire, C. Ciuti, and L. J. Sham, cond-mat/0302088 vl.
[11] M. Tanaka, Semicond. Sci. Technol. **17**, 327 (2002).
[12] For similar current density, temperature, and applied field conditions, samples with doping 6×10^{16}, 8×10^{16}, and 1×10^{17} cm^{-3} all showed maximum effective nuclear fields of ~0.35–0.45 T. The magnitude of electron spin accumulation that occurs over this doping range does not vary widely. A sample with doping 1×10^{18} cm^{-3} showed greatly reduced transverse spin lifetime and negligible nuclear spin polarization.
[13] J. Stephens *et al.*, Phys. Rev. B **68**, 041307(R) (2003).
[14] *Optical Orientation*, edited by F. Meier and B. P. Zakharchenya (North-Holland Physics Publishers, New York, 1984).
[15] J. Strand *et al.*, Phys. Rev. Lett. **91**, 036602 (2003).
[16] S. A. Crooker *et al.*, Phys. Rev. Lett. **77**, 2814 (1996).
[17] The pump/probe intensity is sufficiently small to not substantially alter the nuclear polarization.
[18] D. Paget, G. Lampel, B. Sapoval and V. I. Safarov, Phys. Rev. B **15**, 5780 (1977).
[19] We note that in some cases for the Hanle-MOKE measurements, we observe some asymmetry in the magnitude of the positive and negative peaks of the measured curves. This could be an artifact due the Hall effect, or to a small deviation of the initial direction of the spin from the sample plane. Nevertheless, we use Eq. (1) to fit the measured curves, effectively averaging out the asymmetry.
[20] A. Abragam, *Principles of Nuclear Magnetism* (Oxford University Press, Oxford, 1961).
[21] This simplified model is meant to mimic the spin dependence in the ferromagnet; the spin dependence in the reflection and transmission coefficients and the magnitude of the polarization should be similar to what the model predicts if realistic band structure were used.
[22] GaAs: effective mass $m^* = 0.07$, mobility $\mu = 3000$ cm^2/V s, doping $n = 8 \times 10^{16}$ cm^{-3}; MnAs: $m^* = 1$, spin-up potential $U_{fm}^\uparrow = 3.0$ eV, spin-down potential $U_{fm}^\downarrow = 1.5$ eV; Schottky barrier height: $U_b = 0.8$ eV.